Spectroscopic Studies of the Intermolecular Interactions of a Bis-Azo Dye, Direct Blue 1, on Di- and Trimerization in Aqueous Solution and in Cellulose

Laurence C. Abbott,[†] Stephen N. Batchelor,[‡] John Oakes,[‡] John R. Lindsay Smith,[†] and John N. Moore*,[†]

Department of Chemistry, The University of York, Heslington, York, YO10 5DD, U.K., and Unilever Research, Port Sunlight, Quarry Road East, Bebington, Wirral, CH63 3JW, U.K.

Received: April 2, 2004; In Final Form: June 9, 2004

The intermolecular interactions of the bis-azo dye Direct Blue 1 (Chicago Sky Blue 6B) have been studied as a function of concentration in aqueous solution and in cellophane using UV−visible absorption, NMR, and resonance Raman spectroscopy. UV−visible spectroscopy indicates that dimerization occurs in aqueous solution ($K_{dim} \approx 77\,000$ dm^3 mol^{-1} at $I = 0.01$) and that it occurs more readily at higher ionic strength, where trimerization also occurs ($K_{dim} \approx 580\,000$ dm^3 mol^{-1} and $K_{trim} \approx 2700$ dm^3 mol^{-1} at $I = 0.1$); the driving force is enthalpic rather than entropic ($\Delta H_{dim} \approx -53$ kJ mol^{-1} and $\Delta S_{dim} \approx -90$ J K^{-1} mol^{-1} at $I = 0.01$). Dimerization occurs much less readily in cellophane ($K_{dim} \approx 42$ dm^3 mol^{-1}) than in aqueous solution, indicating that strong dye−cellulose interactions compete effectively with dye−dye interactions. NMR spectroscopy indicates that Direct Blue 1 molecules interact by π-stacking at the central biphenyl group, while resonance Raman spectroscopy indicates that the internal structure and bonding of the monomers is essentially retained on stacking. The UV−visible spectra are consistent with this interpretation, and the application of exciton theory indicates that stacking results in angles between adjacent molecules which are different in the dimer ($\theta \approx 84°$) and trimer ($\theta \approx 58°$); they are attributed to geometries which minimize the repulsion between charged naphthylsulfonate groups.

Introduction

The advent of new technologies has stimulated a resurgence of interest in the chemistry and photochemistry of dyes in solution and on surfaces, extending from the more traditional field of textiles dyeing to new ink-jet printing techniques and biochemical applications.[1,2] One important area of study is that of intermolecular interactions, both between identical dye molecules and between dye molecules and molecular surfaces ranging from those provided by cellulose, synthetic polymers, and microporous media, to those provided by proteins.

Direct dyes are generally large azo dyes, containing two or more azo groups, which have sulfonate groups that provide solubility in water. They are so named because their high substantivity for cellulose enables direct dyeing by simple adsorption processes, due to the total strength of their intermolecular interactions with this substrate.[3] The major application of these dyes is in the dyeing of textiles and papers, but they are now being used in a developing range of biochemical assays for amyloid and other proteins, and they also have the potential for pharmaceutical use in the treatment of HIV and neurodegenerative diseases such as Alzheimer's and scrapie.[4,5] This class of dyes provides an important case for the study of competitive intermolecular interactions. Azo dyes, in general, are well known to form dimers or higher aggregates at high concentrations in solution,[6] due to the presence of dye−dye intermolecular interactions. Direct azo dyes, in particular, are also able to form the relatively strong dye−substrate intermolecular interactions that have resulted in their wide range of applications.

The aggregation of azo dyes in aqueous solution has received significant attention,[6] and a variety of UV−visible, NMR, light scattering, and other techniques has been applied.[7−19] The nature of aggregation, and indeed whether it occurs at all, is strongly dependent on the structure of each particular dye. Thermodynamic parameters have been reported in many cases, and it is generally accepted that aggregation is promoted in aqueous solutions of high ionic strength.[6,13,15] Few kinetic parameters have been reported for azo dyes,[20] although the relatively long-term "aging" that can be observed over many hours as some dyes form colloids has been described.[9] The question of whether dimers or higher aggregates form under various conditions has been debated for several specific azo dyes; small mono-sulfonated mono-azo dyes containing a trifluoromethyl group that facilitates ^{19}F NMR probing, including some which can form liquid crystals, have been the subject of a number of reports.[10−12,14,18,19] The alignment of molecules within dimers or higher aggregates has generally been proposed on the basis either of NMR spectra or of UV−visible spectra interpreted by exciton theory.[7−12,15−19]

Detailed, quantitative reports of aggregation to date have generally focused on small, mono-azo dyes in solution. However, the increasing range of applications of direct dyes means that there is now a need to extend such studies to more complex, multi-azo systems. In particular, it is important to understand the thermodynamic and structural factors that determine the nature of dye−dye intermolecular interactions in these large molecules, and how they may be affected by competitive interactions with the molecular surfaces to which they may be applied. Cellulose remains the most widely used substrate for these dyes; it provides a microporous medium consisting of

[†] The University of York.
[‡] Unilever Research.

10.1021/jp0485542 CCC: $27.50
Published on Web 08/11/2004

polysaccharide chains arranged into crystalline and amorphous regions with pores of ca. 1−3 nm dimension where binding occurs.[21]

We recently reported NMR, UV−visible, IR, and resonance Raman spectroscopic studies of the direct dye Direct Blue 1 (Chicago Sky Blue 6B; below) in aqueous and nonaqueous solvents, and in the microporous cellulose environments of cellophane and cotton.[22] This work demonstrated that Direct Blue 1 is present as a hydrazone tautomer in these environments, and that it is present as a monomer in DMSO, in DMF, and at low dye concentrations in water and in cellulose. The studies also revealed aspects of the intramolecular hydrogen-bonding interactions within the monomer, and of the intermolecular interactions between the monomer and solvent or cellulose molecules.

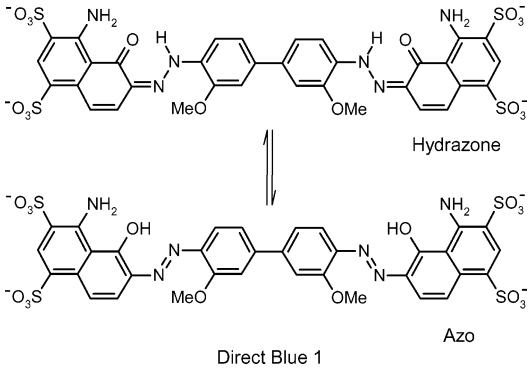

In the present study, we have addressed dye−dye intermolecular interactions of Direct Blue 1, and how these are affected by deposition into cellulose. We report UV−visible, NMR, and resonance Raman studies across a range of concentrations in aqueous solution and in cellophane, including studies of the effect of ionic strength and temperature. The UV−visible spectra demonstrate that aggregation occurs, and their analysis provides information on aggregation numbers, thermodynamic parameters, and molecular orientation. The NMR spectra provide evidence for the locations of the intermolecular interactions within the aggregates, while the resonance Raman spectra report on the effect of aggregation on internal structure and bonding. The UV−visible and resonance Raman data from cellophane samples provide direct evidence of the effects of the cellulose environment on these aggregation properties.

Experimental Section

Materials. Direct Blue 1 (Aldrich) was purified as described previously,[22,23] H_2O was freshly deionized, and D_2O, DMSO-d_6, and DMF-d_7 (Goss Scientific) were used without further purification. The ionic strengths of dye solutions were controlled by dilution with NaCl solutions of appropriate concentrations. Small (ca. 1 × 2 cm) pieces of cellophane film (Sigma, measured thickness 45 μm) were dyed by soaking in a dye solution at room temperature for ca. 30 min and then dried between lint-free tissues with a weight placed on top to prevent wrinkling of the film. The concentrations of the dye in cellophane were estimated from the measured absorption spectra and path length (45 μm) by assuming that the absorption coefficient at the peak of the long-wavelength visible band in cellophane (ca. 656 nm) was the same as the peak of the visible monomer band in aqueous solution (ca. 620 nm). The cellophane had a measured density of 1.25 kg dm^{-3} which, along with a molar mass of 933 g mol^{-1} for Direct Blue 1, gives conversion factors from concentration to loading of 1 mol dm^{-3} ≈ 0.8 mol kg^{-1} ≈ 0.75% w/w (Direct Blue 1/cellophane). This concentration estimate treats cellophane as a homogeneous bulk medium (like water), rather than as a microporous medium; for cellophane, which is a reconstituted form of cellulose, the amorphous region that may be accessible to dyes such as Direct Blue 1 comprises ca. 70% of the total volume.[21]

Methods. UV−visible absorption spectra of freshly prepared solutions were recorded using either a Hitachi U-3000 or a Hitachi U-3010 spectrophotometer with either 10-cm, 1-cm, 1-mm, or 102-μm (measured) fixed path length quartz cells (Hellma), or by transmittance directly through cellophane samples, at a temperature of 298 ± 1 K. Resonance Raman (RR) spectra were recorded at 293 K using the 530.9-nm line from a Kr^+ ion laser (Coherent Innova-90).[22] 1D- and 2D-^{1}H and ^{13}C NMR spectra were recorded at 300 K using a Bruker AMX-500 spectrometer and were calibrated against residual protiated solvent resonances and processed using XWIN NMR (Bruker). Data analysis was performed using either SPSS (SPSS, Inc.) for nonlinear regression or software written in-house; uncertainties are reported as $\pm 2\sigma$ (σ = standard deviation), that is, as 95% confidence limits. Some of the mathematical manipulations needed in the trimerization and exciton theory analyses were performed or confirmed using Maple (Waterloo Maple, Inc.).

Results and Analysis

UV−Visible Absorption Spectroscopy. UV−visible absorption spectra of Direct Blue 1 in aqueous solution were recorded from two sets of solutions at different ionic strengths (I = 0.01 and 0.1), across a range of ca. 20 total dye concentrations (c_{tot} = 2 × 10^{-7} to 1 × 10^{-3} and 1 × 10^{-2} mol dm^{-3}, respectively), with both sets of solutions held at constant pH (7.1) and temperature (T = 298 ± 1 K). The spectra were recorded in the peak absorbance range of A = 0.1−2.5 by using cells of appropriate path length l, and sample spectra are shown in Figure 1, plotted as ($A/c_{tot}l$) values. The changes in the profiles of the spectra with concentration are small but significant, and they indicate that aggregation occurs: the largest changes occur at ca. 670 nm, on the red-edge of the main visible band.

The simplest form of aggregation is that of a monomer−dimer equilibrium,[7−19] given by eq 1, where M is the monomer and K_{dim} is the dimerization constant.

$$\mathrm{M} + \mathrm{M} \rightleftharpoons \mathrm{M}_2 \qquad K_{\mathrm{dim}} = \frac{[\mathrm{M}_2]}{[\mathrm{M}]^2} \tag{1}$$

The experimental data at a specific wavelength can be analyzed with eq 2 (see Appendix SA1), where ϵ_{mon} and ϵ_{dim} are the absorption coefficients (at that wavelength) of the monomer and dimer, respectively:

$$\frac{A}{c_{\mathrm{tot}}l} = \frac{\sqrt{1 + 8K_{\mathrm{dim}}c_{\mathrm{tot}}} - 1}{4K_{\mathrm{dim}}c_{\mathrm{tot}}}\left(\epsilon_{\mathrm{mon}} - \frac{\epsilon_{\mathrm{dim}}}{2}\right) + \frac{\epsilon_{\mathrm{dim}}}{2} \tag{2}$$

Figure 1 (inset) shows a fit of eq 2 to the data at 670 nm from Direct Blue 1 at the two ionic strengths, with the fitted K_{dim} values given in Table 1. The absorption coefficients are well defined by the plateaus at low and high concentrations and have narrow uncertainty limits (Table SA1): the value of ϵ_{mon} is the same at the two ionic strengths, and that of ϵ_{dim} is similar, indicating that the analysis at this wavelength defines the same

TABLE 1: Equilibrium Constants (298 K) and Thermodynamic Data for Aggregation of Direct Blue 1 in Aqueous Solution[a]

medium	I	model[b]	K_{dim}/ 10^3 dm^3 mol^{-1}	K_{trim}/ 10^3 dm^3 mol^{-1}	ΔG_{dim}[c]/ kJ mol^{-1}	ΔG_{trim}[c]/ kJ mol^{-1}	ΔH_{dim}/ kJ mol^{-1}	ΔS_{dim}/ J K^{-1} mol^{-1}	ΔG_{dim}[d]/ kJ mol^{-1}
aqueous	0.01	M ⇌ D	77 ± 42		−28 ± 2		−53 ± 3	−90 ± 11	−26 ± 6
aqueous	0.1	M ⇌ D	570 ± 200		−33 ± 1		−90 ± 10	−193 ± 32	−32 ± 20
aqueous	0.1	M ⇌ D ⇌ T	580	2.7	−33	−20			
cellophane		M ⇌ D	0.042		−9				

[a] Uncertainties are $\pm 2\sigma$, obtained from nonlinear regression analysis. [b] M = monomer, D = dimer, T = trimer. [c] Calculated from K values at 298 K. [d] Calculated at 298 K from ΔH_{dim} and ΔS_{dim} values.

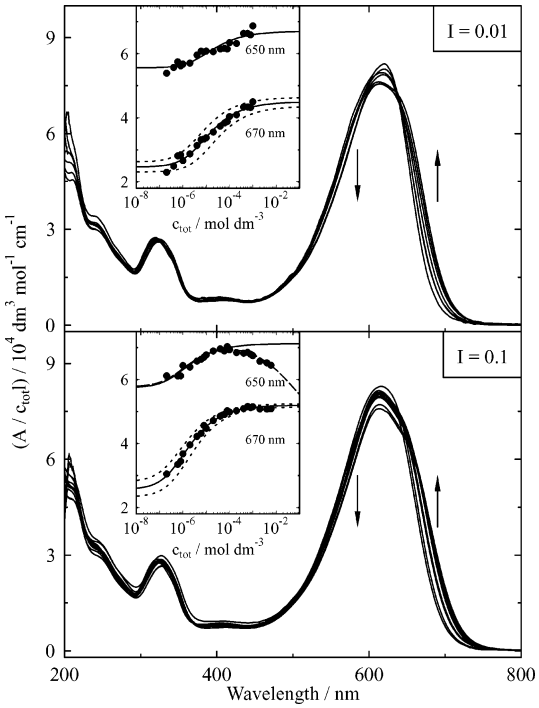

Figure 1. Sample UV−visible absorption spectra of Direct Blue 1 as a function of dye concentration in aqueous solution at pH = 7.1, T = 298 ± 1 K, and at I = 0.01 (upper) and 0.1 (lower); the arrows show changes with increasing dye concentration. Insets: fits to eq 2 (solid lines) with 95% confidence limits (dotted lines; 670 nm data), and to eq 4 (dashed line; 650 nm data at I = 0.1); details in Appendix SA1.

monomer and dimer species. Although the uncertainty limits in the dimerization constants are moderately large (Table 1), because the change in the normalized absorbance with concentration is relatively small, it is clear that their values differ significantly at these two ionic strengths.

The use of eq 2 to analyze data at wavelengths other than ca. 670 nm gave acceptable fits for the I = 0.01 data set (Figure 1), giving K_{dim} values within the uncertainty range obtained from the analysis at 670 nm and indicating that the monomer−dimer model is applicable to the whole data set at low ionic strength. By contrast, eq 2 gave poor fits for the I = 0.1 data set at some wavelengths, as is shown in Figure 1 for data at 650 nm (solid line), indicating that the monomer−dimer model is not applicable to solutions at higher ionic strength and higher concentrations.

The next level of aggregation beyond dimer formation is trimer formation,[24] as given by eq 3, with an additional equilibrium constant, K_{trim}.

$$M_2 + M \rightleftharpoons M_3 \qquad K_{trim} = \frac{[M_3]}{[M_2][M]} \tag{3}$$

The experimental data at a specific wavelength can be analyzed with eq 4 (Appendix SA1), where ϵ_{trim} is the absorption coefficient (at the analysis wavelength) of the trimer.

$$\frac{A}{c_{tot}l} = \epsilon_{mon}\frac{c_{mon}}{c_{tot}} + \epsilon_{dim}K_{dim}\frac{c_{mon}^{\ 2}}{c_{tot}} + \epsilon_{trim}K_{dim}K_{trim}\frac{c_{mon}^{\ 3}}{c_{tot}} \tag{4}$$

A fit of eq 4 to the data at 650 nm from Direct Blue 1 at I = 0.1 is shown as the dashed line in Figure 1 (inset), with the fitted values given in Tables 1 and SA1.

The values of ϵ_{mon} and ϵ_{dim} at 650 nm are well defined from the fit to eq 2 at I = 0.01 and from the fit to eq 4 at I = 0.1; ϵ_{mon} is the same at both ionic strengths, and ϵ_{dim} is closely similar (Table SA1), indicating that the respective analyses at this wavelength define the same monomer and similar dimer species. The fit to eq 4 at I = 0.1 also gives ϵ_{trim} at 650 nm, and, importantly, it provides estimates of K_{dim} and K_{trim} (Table 1). The value of K_{dim} obtained from analyzing the 650 nm data with eq 4 is the same as that obtained from analyzing the 670 nm data with eq 2 (Table SA1). These consistent values indicate that the K_{dim} analysis is robust but that the sensitivity of the absorbance to trimer formation varies with wavelength, as may be expected when the overlap of the absorption bands of different species varies with wavelength. The good fit to the monomer−dimer−trimer model indicates that it is applicable to the data at higher ionic strength, showing an increasingly significant concentration of trimers with increasing concentration and a value of K_{trim} that is ca. 200 times smaller than that of K_{dim}.

In principle, the aggregation model can be extended by adding further equilibria for tetramers and higher aggregates, eq 5, each with a distinct equilibrium constant.

$$M_3 + M \rightleftharpoons M_4 .... \qquad M_{n-1} + M \rightleftharpoons M_n \tag{5}$$

It is possible to determine each equilibrium constant when the number of molecules within an aggregate is small because monomers, dimers, and trimers typically have overlapping but distinguishable UV−visible spectra.[24,25] However, the successive changes between dimers, trimers, tetramers, etc., typically become increasingly small, and their spectra can be obtained only by the analysis of spectra from mixtures because these species cannot generally be isolated. The analysis of a spectroscopic data set should reasonably be constrained to that for species with distinguishable spectra. Consequently, individual equilibrium constants are difficult to determine when the aggregate number is large, and analyses in such cases are often based on a general monomer−n-mer model with the assumption either that the equilibrium constants are identical for all steps[18,19,26] or that two equilibrium constants define the entire process.[27] The analysis presented above is based on three species with distinguishable spectra, and so we have applied a further test of this model using factor analysis,[28] which is a powerful statistical technique for determining the number of components responsible for a data set that can be applied either as a pure statistical analysis (i.e., model-free) or in combination with an assumed model that provides some constraints (e.g., monomer−

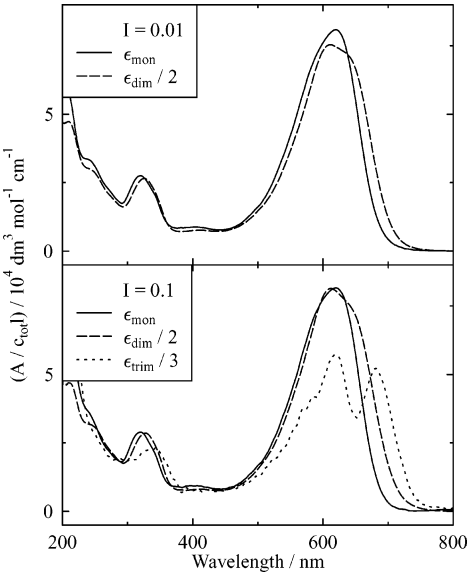

Figure 2. UV−visible absorption spectra of the monomer (ϵ_{mon}), dimer (ϵ_{dim}), and trimer (ϵ_{trim}) of Direct Blue 1 in aqueous solution, obtained by fitting the full data sets in Figure 1: at $I = 0.01$ (upper) to eq 2 with a fixed value of $K_{dim} = 7.7 \times 10^4$ dm^3 mol^{-1}; and at $I = 0.1$ (lower) to eq 4 with fixed values of $K_{dim} = 5.8 \times 10^5$ and $K_{trim} = 2.7 \times 10^3$ dm^3 mol^{-1}; band positions in Table SA2. The spectra are scaled per monomer unit: ϵ_{mon}, $\epsilon_{dim}/2$, and $\epsilon_{trim}/3$.

dimer model). Factor analysis with a monomer−dimer model has been applied to dye aggregation in the past,[9] and we have recently developed a series of programs for its application to spectroscopic data sets using current algorithms.[29] Applying model-free abstract factor analysis to the spectra at different concentrations, and including an algorithm for multiple sources of errors[30] to reflect the different sample cells used, results in an indicator function[28] which indicates that the data set at high ionic strength arises from three factors. This independent and model-free analysis provides additional justification for the application of a model that defines three distinguishable species, that is, monomer, dimer, and trimer, for the data from Direct Blue 1 at $I = 0.1$.[31]

The spectra of the monomer, dimer, and trimer were obtained by fitting the full data sets at each ionic strength across all wavelengths. For the data at $I = 0.01$, constraining to $K_{dim} = 7.7 \times 10^4$ dm^3 mol^{-1} and fitting eq 2 to the full data set at each wavelength gave the monomer and dimer spectra shown in Figure 2. This analysis was found to be insensitive to the exact value of K_{dim}, as was expected because the well-defined plateaus at low and high concentrations define the spectra, with sample fits using constraints between $2-10 \times 10^4$ dm^3 mol^{-1} giving monomer and dimer spectra almost identical to those shown in Figure 2. Similarly for the data at $I = 0.1$, constraining to $K_{dim} = 5.8 \times 10^5$ and $K_{trim} = 2.7 \times 10^3$ dm^3 mol^{-1} and fitting eq 4 to the full data set at all wavelengths gave the monomer, dimer, and trimer spectra (Figure 2). The monomer spectra obtained from these two data sets and analyses are almost identical, and they match that obtained experimentally at low concentration and low ionic strength; the dimer spectra are also closely similar. It is evident that the three species have distinct UV−visible absorption spectra, and the band positions and absorption coefficients obtained from the spectra in Figure 2 are reported in Table SA2.[33] These spectra also illustrate the wavelengths where significant changes occur, and which are used for analysis (Figure 1, insets): the largest change between monomer and dimer is an increase at ca. 670 nm, on the red shoulder of the main band and close to an isosbestic point between dimer and trimer; and the largest change between dimer and trimer is at ca. 650 nm, which shows a large increase from monomer to dimer and an even larger decrease from dimer to trimer.

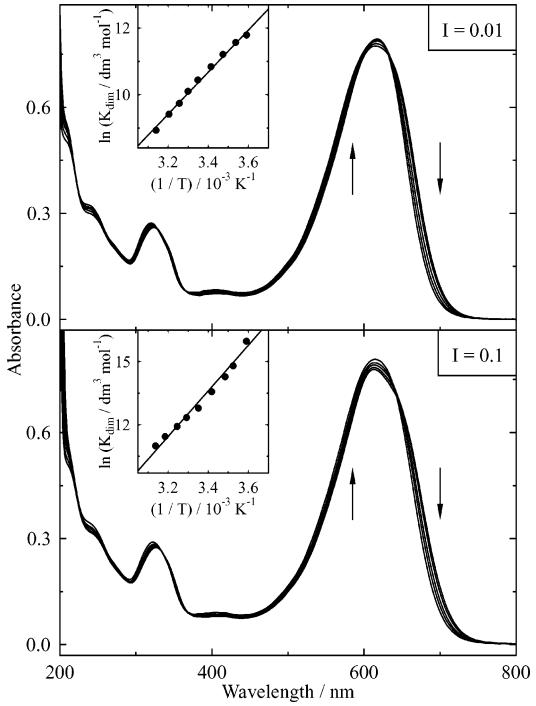

Figure 3. Sample UV−visible absorption spectra of Direct Blue 1 in aqueous solution at temperatures in the range of 5−45 °C at $I = 0.01$ (upper) and $I = 0.1$ (lower), both at 1×10^{-5} mol dm^{-3} in a 1-cm path length cell; the arrows show changes with increasing temperature. The spectra are corrected for volume changes with temperature.[34] Insets: temperature-dependent K_{dim} values fitted to eq 6.

UV−visible absorption spectra of Direct Blue 1 in aqueous solution were recorded at temperatures from 5 to 45 °C at both low and high ionic strength (Figure 3). The changes in the profiles of the spectra indicate that the positions of the aggregation equilibria shift with temperature, with the largest changes occurring at ca. 670 nm and isosbestic points as observed with changes in concentration (Figures 1 and 2).[35] The fractions of trimer present in these samples were very low (<2% at high ionic strength; see Figure SA1), and so the data at both ionic strengths were analyzed using the monomer−dimer model. The spectra observed at each temperature were fitted to eq SA2, using the calculated monomer and dimer spectra (Figure 2), to obtain the monomer and dimer concentrations and hence, from eq 1, a K_{dim} value at each temperature for each sample. Further analysis by eq 6 (Figure 3, insets) gave values for the change in enthalpy ΔH_{dim} and entropy ΔS_{dim} on dimerization (Table 1).

$$\ln K_{dim} = \frac{-\Delta H_{dim}}{RT} + \frac{\Delta S_{dim}}{R} \qquad (6)$$

The temperature-dependent data indicate that the dimerization reaction is exothermic but entropically unfavorable, becoming more exothermic and more entropically unfavorable at higher ionic strength.

NMR Spectroscopy. ^{1}H NMR spectra of Direct Blue 1 in D_2O were recorded at concentrations between 5×10^{-4} and 1×10^{-2} mol dm^{-3}, as is shown in Figure 4. The relatively low sensitivity of the NMR technique precluded observations at concentrations where only the monomer is present in D_2O, and so spectra in DMSO-d_6 and DMF-d_7, where the dye is present

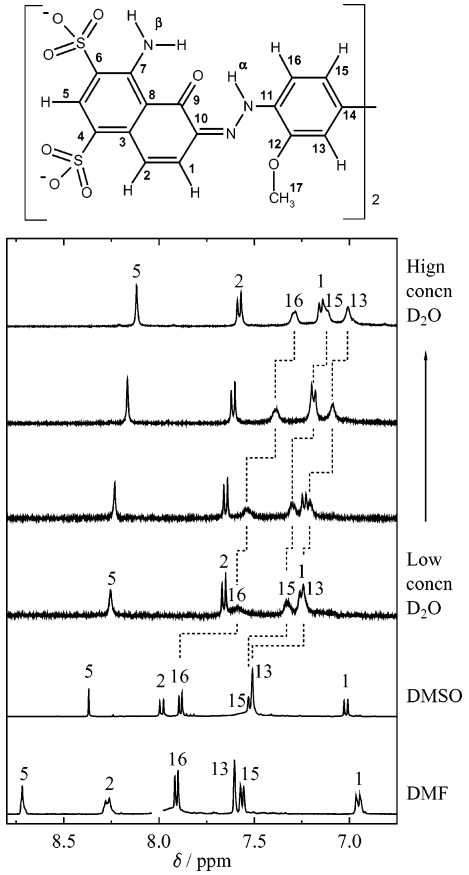

Figure 4. ^{1}H NMR spectra (aromatic region) of Direct Blue 1 in D_2O at 1×10^{-2}, 5×10^{-3}, 1×10^{-3}, and 5×10^{-4} mol dm^{-3} at $I \leq 0.01$ (no NaCl added), and in DMSO-d_6 and DMF-d_7 at 3×10^{-2} mol dm^{-3} (resonance from residual DMF-h_7 at ca. 8 ppm removed); dashed lines show changes in resonances from H13, H15, and H16. The structure shows the atom numbering for assignments.

as a monomer even at high concentrations,[22] were recorded for comparison (Figure 4). Table SA3 (Appendix SA1) lists the chemical shifts, splittings, and assignments according to the atom numbering in Figure 4,[22] along with differences in chemical shifts between different samples. The data can be interpreted in terms of aggregation and solvation effects that act differently on protons within the biphenyl and naphthyldisulfonate groups.

The changes in the positions of the resonances with concentration in D_2O are characteristic of aggregation, with rapid exchange on the NMR time scale giving average positions that depend on the relative concentrations of the species in dynamic equilibrium.[10−12,19,26,37] The largest changes with increasing concentration are upfield shifts in the resonances from H13, H15, and H16 on the central biphenyl group. These resonances also show large upfield shifts and considerable broadening on going from either DMF or DMSO (monomer dye) to D_2O (aggregated dye), to the extent that the doublet splittings observed for H15 and H16 in DMF and DMSO are lost in D_2O. By contrast, the positions and widths of these resonances change relatively little between DMF and DMSO.

The resonances from H1, H2, and H5 on the naphthyldisulfonate groups show comparatively small upfield shifts with concentration in D_2O, and they do not show considerable broadening on going from DMF or DMSO to D_2O. However, these resonances do show relatively large changes in position and width between DMF and DMSO, indicating that they are more sensitive to the solvent environment than those from H13, H15, and H16. The changes between DMF and DMSO are larger for H2 and H5 than for H1, suggesting that the effect may arise from the close proximity of these protons to the sulfonate groups.

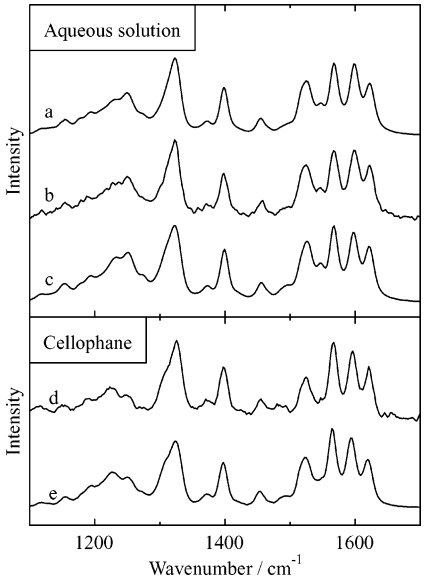

Figure 5. Resonance Raman spectra, obtained at an excitation wavelength of 530.9 nm, of Direct Blue 1: in aqueous solution at (a) 1×10^{-4} and (b) 1×10^{-2} mol dm^{-3}, and at (c) 1×10^{-4} mol dm^{-3} in 1 mol dm^{-3} NaCl solution; in cellophane at (d) 5×10^{-4} and (e) 2×10^{-2} mol dm^{-3}.

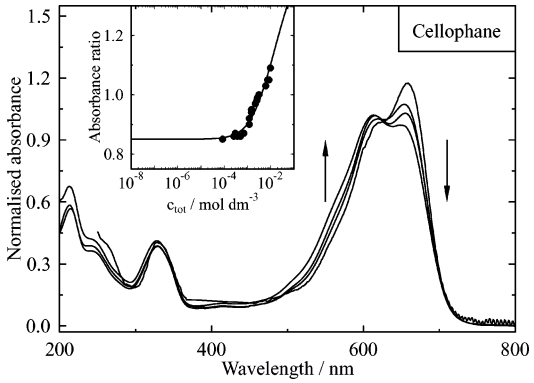

Figure 6. Sample UV−visible absorption spectra of Direct Blue 1 in cellophane at $T = 298 \pm 1$ K as a function of dye concentration, scaled to the absorbance at 617 nm; the arrows show the change with increasing concentration. Inset: fit to eq 7 for $\lambda_1 = 612$ nm and $\lambda_2 = 656$ nm; details in Table SA4.

Resonance Raman Spectroscopy. Resonance Raman spectra of Direct Blue 1 in aqueous solution were recorded at concentrations from 1×10^{-4} to 1×10^{-2} mol dm^{-3}, and at a very high ionic strength of $I = 1$. The spectra were found to be essentially independent of both concentration and ionic strength, as illustrated in the upper plot of Figure 5.

Spectroscopic Studies of Cellulose Samples. UV−visible absorption spectra of Direct Blue 1 in cellophane were recorded at ca. 20 total dye concentrations from $c_{tot} = 1 \times 10^{-4}$ to 1×10^{-2} mol dm^{-3} (estimated concentrations; see Experimental Section) at a temperature of 298 ±1 K. Absorbance measurements were made in the range of $A = 0.1-3.0$: the lowest concentrations were studied by using stacks of up to three individual cellophane pieces; the highest observable concentration was limited by the transmittance through the minimum path length of 45 μm for a single cellophane piece. Sample data are shown in Figure 6, scaled to the absorbance at 617 nm (see below). The change in profile with concentration is indicative

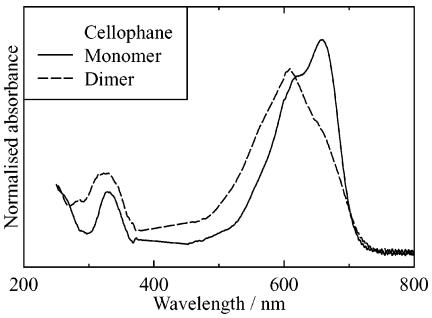

Figure 7. Estimated UV−visible absorption spectra of Direct Blue 1 in cellophane: monomer (observed spectrum from a stack of five films at $c_{tot} = 1 \times 10^{-5}$ mol dm^{-3}, with sloping background due to cellophane scattering subtracted); dimer (from a scaled subtraction of the monomer spectrum from that of a single-film sample at $c_{tot} = 8 \times 10^{-3}$ mol dm^{-3}; see text).

of aggregation in cellophane, with the spectrum at high concentration being similar to that of the dimer in aqueous solution (Figure 2).

The spectra from the cellophane samples were analyzed by a monomer−dimer model. For aqueous samples, the analysis of $(A/c_{tot}l)$ data with eq 2 is appropriate because accurate c_{tot} values are known from experiment; for the cellophane samples, however, it is more appropriate to analyze the measured absorbance values directly because the c_{tot} values are estimated. In this case, the ratio of the measured absorbances at two wavelengths within the same spectrum give appropriate data to estimate the relative contribution of two species at each concentration. Equation 7, derived from eq 2, gives this ratio at any two wavelengths, λ_1 and λ_2, where ϵ_{mon1} and ϵ_{mon2}, and ϵ_{dim1} and ϵ_{dim2}, are the monomer and dimer absorption coefficients, respectively, at these two wavelengths.

$$\frac{A_1}{A_2} = \frac{(\sqrt{1 + 8K_{dim}c_{tot}} - 1)(2\epsilon_{mon1} - \epsilon_{dim1}) + 4K_{dim}c_{tot}\epsilon_{dim1}}{(\sqrt{1 + 8K_{dim}c_{tot}} - 1)(2\epsilon_{mon2} - \epsilon_{dim2}) + 4K_{dim}c_{tot}\epsilon_{dim2}} \quad (7)$$

Figure 6 (inset) shows a fit of eq 7 to the data from Direct Blue 1 in cellophane, at wavelengths of $\lambda_1 = 612$ nm and $\lambda_2 = 656$ nm which are the two maxima in the observed spectra, with the parameters obtained from the fit given in Tables 1 and SA4. The $(\epsilon_{mon1}/\epsilon_{mon2})$ value is well defined from the plateau at low concentration, whereas the $(\epsilon_{dim1}/\epsilon_{dim2})$ and K_{dim} values have large uncertainties because the limiting (A_1/A_2) value at high concentration is not well defined due to the maximum concentration of 10^{-2} mol dm^{-3} that could be studied with the thickness of film available. However, it is clearly evident from the concentration dependence that the dimerization constant of Direct Blue 1 is much lower in cellophane (Figure 6 inset) than it is in aqueous solution (Figure 1 inset).

The spectrum observed at low concentration in cellophane (Figure 7), from a stack of films, can be assigned to that of the monomer. The spectrum of the dimer in cellophane was estimated (Figure 7) by making a scaled subtraction of the monomer spectrum from the spectrum of a sample at high concentration, using eqs 1, SA1, and SA2 along with c_{mon} and c_{dim} values obtained using $K_{dim} = 42$ dm^3 mol^{-1}. Although the spectrum of the dimer in cellophane is estimated with some uncertainty, it is similar to that of the dimer in aqueous solution (Figure 2); the estimated isosbestic point at 617 nm in cellophane was used to scale the experimental data in Figure 6.

Resonance Raman spectra of Direct Blue 1 in cellophane were recorded at concentrations from 5×10^{-4} to 2×10^{-2} mol dm^{-3}. The spectra were found to be essentially independent of concentration, as is shown in the lower plot of Figure 5.

Discussion

The analysis of the UV−visible data provides strong evidence for the existence of discrete monomer, dimer, and trimer forms of Direct Blue 1 in aqueous solution, and for monomer and dimer forms in cellulose, and it determines the thermodynamic parameters. The NMR, UV−visible, and RR spectra together provide complementary information on aggregate structures, and these will be discussed prior to further discussion of the thermodynamics.

Structures. The large shifts and broadening of the NMR resonances of protons H13, H15, and H16 on going from monomer to dimer in solution, along with their shifts with concentration (Figure 4; Table SA3), suggest that the central biphenyl group is the main site of intermolecular interaction in Direct Blue 1 aggregates, with the upfield shifts being indicative of π-stacking.[26,37] This interpretation is consistent with the molecular structure of Direct Blue 1: the central biphenyl group is uncharged and relatively hydrophobic, and it may be expected to provide a favorable site for $\pi-\pi$ interactions with the concomitant release of water molecules ordered around it. By contrast, the charged naphthyldisulfonate groups may be expected to minimize intermolecular dianion−dianion interactions by locating themselves away from each other within the octa-anionic dimer. It may be inferred that trimer formation will then involve a third molecule stacking at the central biphenyl group.

The main UV−visible band of Direct Blue 1 shows a blue shift on aggregation that is characteristic of π-stacking,[7−16,18,19,24,25] consistent with the interpretation of the NMR data. Exciton theory[38,39] predicts that a monomer excited state splits into two levels in a dimer, with oscillator strengths f_1 and f_2 for transitions to the lower and higher energy levels at ν_1 and ν_2, respectively, related to the angle θ between the transition dipoles of the two monomers by eq 8.

$$\theta = 2\tan^{-1}\sqrt{\frac{f_1\nu_2}{f_2\nu_1}} \quad (8)$$

The difference in energy $\Delta\nu_{12}$ (cm^{-1}) between the two levels, which is twice the interaction energy U between the two monomers, is related by eq 9 to the separation distance R (Å) and the oscillator strength f_m for the monomer transition at ν_m (cm^{-1}), with the exact form of the relationship depending on the structure of the dimer according to a geometric factor, x.

$$\Delta\nu_{12} = 2U = \frac{2.14 \times 10^{10} f_m}{\nu_m R^3} x \quad (9)$$

For a stacked dimer, three cases can be considered, shown below:

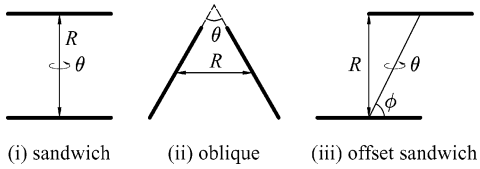

(i) a "sandwich" dimer with a central twist angle ($x = \cos\theta$); (ii) an "oblique" dimer with an angle between the molecular

TABLE 2: Band Positions and Splittings (cm^{-1}), Interaction Energies (cm^{-1}), Relative Oscillator Strengths, Angles (deg), and Distances (Å) Estimated for the Direct Blue 1 Dimer and Trimer in Water and in Cellophane

medium	I	species	ν_1	ν_2	ν_3	$\Delta\nu_{12}$	$\Delta\nu_{23}$	U	U'	f_1/f_2	f_2/f_3	θ	case i[a] R	case ii[b] R	case iii[c] ϕ
aqueous	0.01	dimer	15 314	16 499		1185		+593		0.73		83.1	5.6	12.7	79.9
aqueous	0.1	dimer	15 240	16 473		1233		+617		0.75		84.0	5.2	12.6	80.9
aqueous	0.1	trimer	14 613	16 148	17 387	1535	1239	+980	−98	0.89	1.64	57.8	7.7		66.2
cellophane		dimer	15 097	16 372		1275		+638		0.62		78.6	6.0	11.6	76.6

[a] Sandwich. [b] Oblique. [c] Offset sandwich, calculated for $R = 3.4$ Å.

planes ($x = \cos\theta + 3\sin^2(\theta/2)$); and (iii) an "offset sandwich" dimer in which one of the monomers is displaced horizontally ($x = \cos\theta - 3\cos^2\phi$, where ϕ is the horizontal displacement angle).

The extension of this approach to a stacked trimer shows that the monomer excited state splits into three levels,[40−43] as detailed in Supporting Information Appendix SA2. For a "triple-decker sandwich" trimer in which the separation between two nonadjacent monomers is taken as $2R$ and the angle as 2θ, that is, twice the distance and twice the angle between adjacent monomers, the angle θ is related by eq 10 to the interaction energies U between adjacent monomers (eq 9) and U' between nonadjacent monomers (eq SA16) within the trimer.

$$\theta = \cos^{-1}\left(\frac{4U' \pm \sqrt{16U'^2 + 2U^2}}{2U}\right) \qquad (10)$$

The interaction energies U and U' can be calculated from the observed splittings in the trimer spectrum using eqs SA14 and 15 (see Appendix SA2), and thus the angle θ for a "sandwich" trimer can be calculated from the observed peak positions.

The calculated dimer and trimer spectra of Direct Blue 1 (Figure 2) have been fitted to a sum of Gaussians, as is shown in Figure 8, to enable the positions and relative oscillator strengths of the bands to be estimated. The fitted peak positions of the main components were found to be within 0−70 cm^{-1} (ca. 0−3 nm) of the starting peak positions obtained from the second derivative of the experimental data. Additional bands at shorter wavelength were fixed to the width of the main band and were set to increment in fixed wavenumbers, modeling a vibrational progression.[44] The fitted components labeled 1, 2, and 3 in Figure 8 were used for further calculations: the relative oscillator strengths were estimated from the relative areas under these component bands, and the energy levels of the states were estimated as their peaks (Table 2). The oscillator strength of the monomer was estimated as $f_m = 4.32 \times 10^{-9} \int \epsilon(\nu)\, d\nu = 1.28$, from the area under the visible band of the calculated monomer spectrum from both of the solution samples; this value was also used for the monomer in cellophane.

The results of applying eqs 8−10, as appropriate, are given in Table 2. For the dimer in solution, eq 8 gives an angle of $\theta \approx 84°$ that is insensitive to small changes in the estimates of the relative oscillator strengths;[45] it is evident that it is close to 90° from the similar intensities of the two dimer bands in the raw data. Equation 9 then gives a separation distance of $R \approx 5$ Å for a sandwich model, $R = 13$ Å for an oblique model, and a minimum angle of $\phi \approx 80°$ for an offset sandwich model using $R = 3.4$ Å as an estimate of the closest distance of approach with van der Waals surfaces in contact.[15] The calculated angles and distances suggest strongly that a sandwich rather than an oblique geometry is adopted by the large Direct Blue 1 molecule.[46] The calculated separation distance is moderately sensitive to small changes in the estimated angles and band positions,[47] but the value of ca. 5 Å for the sandwich model is plausible: a value that is slightly greater than the estimated van der Waals contact distance may arise from the biphenyl groups of both monomers being twisted,[48,49] as well as from possible repulsive forces. The offset sandwich model is essentially a small modification to the sandwich model in the case of Direct Blue 1: any offset angle must be >80°, that is, approaching perpendicular, for a separation distance of >3.4 Å.

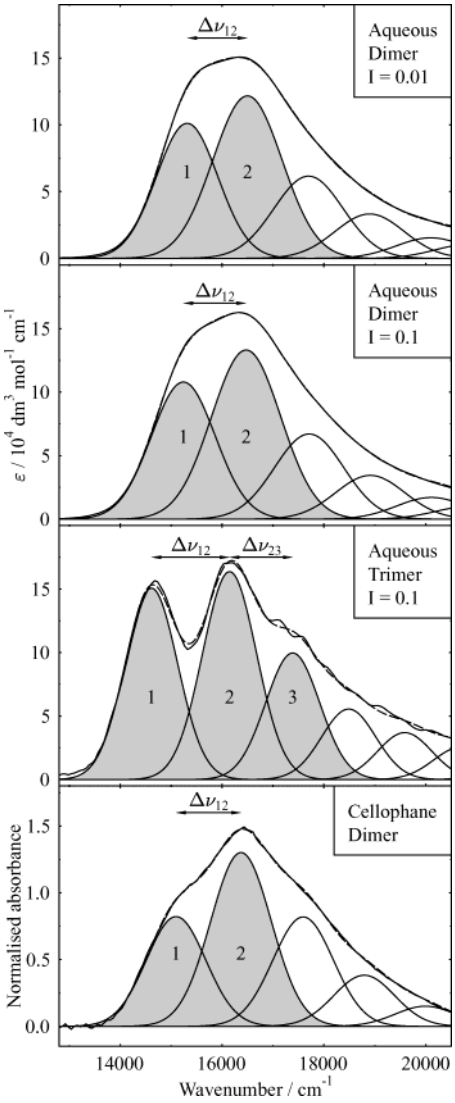

Figure 8. Band-fitting analysis of the calculated monomer, dimer, and trimer spectra of Direct Blue 1 in solution and in cellophane; details in Appendix SA1.

The spectrum of the trimer in solution gives splittings that, from eqs SA14 and 15 and eq 10, yield a twist angle of $\theta = 58°$ for the stacked trimer model, which is considerably smaller than that for the stacked dimer model. Equation 9 then gives a separation distance of $R = 7$ Å for the trimer, which is greater than that in the dimer.

The spectrum of the dimer in cellophane yields an angle of 79° and a separation of 6 Å, which are similar to those determined for the dimer in solution, suggesting that the dimer structure is similar in the two media. The slight further increase from the perpendicular and greater separation distance in cellophane may reflect constraints imposed by the environment, which may include specific competitive intermolecular interactions with cellulose and more general steric effects of the surrounding supramolecular structure.

Overall, analysis by exciton theory suggests that the dimer and trimer of Direct Blue 1 adopt the stacked sandwich structures shown schematically below, as "overhead" views. In the dimer, the monomers are at a twist angle approaching 90° and at a separation approaching contact of the van der Waals surfaces. In the trimer, the twist angle is reduced to ca. 60°, and the monomers are situated slightly further apart. These geometries suggest that the biphenyl group of each monomer provides the main site of intermolecular interaction in the aggregates and that significant repulsion between the pairs of naphthyldisulfonate groups is minimized.

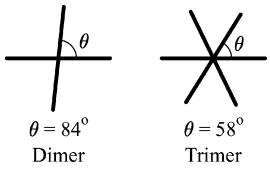

The resonance Raman spectra of Direct Blue 1 are remarkably unchanged on going from monomer to dimer either in solution or in cellophane (Figure 5). Vibrational spectra are most sensitive to changes in internal structure and bonding, and the RR spectrum of the Direct Blue 1 monomer has been shown to report effectively on tautomer composition and on internal and external hydrogen-bonding interactions at the naphthylamino-hydrazone groups.[22] The respective RR spectra indicate that the structure and bonding of the monomer are largely retained on dimerization in each environment. Specifically, they indicate that the dimers comprise two hydrazone monomers, that there is no major disruption of the hydrogen-bonding interactions at the naphthylaminohydrazone groups on dimerization, and that there is no significant inequivalence either between different molecules or between two halves of a single Direct Blue 1 molecule. The absence of any new bands in the fingerprint region is consistent with a π-stacked dimer, for which any new monomer−monomer intermolecular vibrational modes would be expected to occur at very low frequency.[50] Differences between the RR spectra of the monomer of Direct Blue 1 in aqueous solution and cellophane have been assigned to external hydrogen bonding of the naphthylaminohydrazone groups with water and cellulose, respectively:[22] the RR data presented here indicate that the respective external hydrogen bonding with water and cellulose is retained in the dimers.

Together, the NMR, UV−visible, and RR spectra provide consistent evidence that the internal structure and bonding of the Direct Blue 1 monomers are largely retained as they stack at the central biphenyl group to form a dimer in which the axes of the two molecules are close to perpendicular, and a trimer in which the stacking geometry changes to minimize intermolecular repulsion in the stack. The UV−visible and RR spectra indicate that the structure of the Direct Blue 1 dimer in cellophane is similar to that in solution, although the two monomers are slightly more displaced from the perpendicular and from each other than they are in solution, and the intermolecular hydrogen bonding of the molecule with cellulose is retained.

Thermodynamics. The thermodynamic data from solution (Table 1) indicate that the driving force for dimerization of Direct Blue 1 is enthalpic, with an unfavorable decrease in entropy. Although ΔH_{dim} and ΔS_{dim} values vary significantly between the smaller azo dyes that have generally been studied to date, the specific values obtained for Direct Blue 1 lie close to the general trend in enthalpy−entropy correlation observed for a wide range of different dyes,[6] including these smaller azo dyes.

The loss of solvent order around a hydrophobic group can provide the driving force for the dimerization of some dyes, but this is evidently not the case for Direct Blue 1. Although it may be expected that water molecules do form a relatively ordered solvent cage around the hydrophobic biphenyl group, the unfavorable overall entropy change on dimerization indicates that a simple hydrophobic effect may contribute but does not dominate. Rather, the loss of entropy suggests a significant decrease in the overall degrees of motional freedom, which may arise from a significant loss of internal torsional freedom as the two bulky Direct Blue 1 monomers combine.

The exothermic nature of the dimerization indicates that there is significant interaction between the biphenyl groups of the two monomers. The nature of aromatic interactions is of topical interest, in part arising from a drive to understand the interactions that control nucleotide stacking.[50,51] The factors which may contribute to such stacking include electrostatic, induction, and dispersion interactions, with a geometry in which stacked aromatic rings are offset rather than face-to-face being observed most commonly, particularly for larger ring systems.[52] The near-perpendicular orientation of the monomers within the Direct Blue 1 dimer indicated by exciton theory, combined with the actual molecular structure and the likely twisting between the two biphenyl rings within each molecule, is consistent with a stacked geometry in which these rings are in an offset rather than face-to-face orientation.

The dependence of the dimerization constant on ionic strength was studied here principally to confirm the validity of the monomer−dimer model at low concentration and low ionic strength, but it also provides thermodynamic information (Table 1). The higher dimerization constant obtained at higher ionic strength is explained qualitatively by the greater relative stabilization of the more highly charged dimer over the monomer due to the effect of charge-screening. The increase in the magnitude of the enthalpic contribution at higher ionic strength may be attributed to a decrease in repulsion between the charged monomers on dimerization, which may also be reflected by the slightly shorter separation distance and greater twist angle estimated from the dimer spectrum at the higher ionic strength (Table 2).

The dimerization constant of Direct Blue 1 in cellophane is much lower than that in aqueous solution; considering these as bulk media, the relative stabilization of the monomer versus the dimer is higher in cellophane than it is in water. The comparison can also be considered in terms of the interactions of Direct Blue 1 with either the water molecules that solvate the dye in aqueous solution or the cellulose molecules that "solvate", or provide binding sites, in cellophane. Although it might be expected that deposition onto a surface could increase aggregation due to spatial confinement, the microporous cellophane medium evidently provides sufficient monomer binding sites for this not to be a major effect for Direct Blue 1 at moderate concentrations; instead, deposition into the microporous cellulose structure inhibits rather than promotes aggregation. The observation of cellophane dyeing from aqueous

solution indicates that there is a free energy change driving the process, and the observation that deposition into cellulose breaks up aggregates that are present in solution indicates that the intermolecular interactions between a monomer dye and cellulose are strong. A driving force for monomer−cellulose binding which competes with that of ca. −30 kJ mol^{-1} reported here for dimerization of Direct Blue 1 in aqueous solution is consistent with the strong binding properties of direct dyes that are attributed to their multiple intermolecular interactions with cellulose. The relatively small driving force of ca. −9 kJ mol^{-1} for dimerization in cellophane may be attributed to dye−cellulose interactions that compete more strongly with dye−dye interactions in cellophane than the dye−water interactions compete with dye−dye interactions in aqueous solution. EPR studies of TEMPOL probe radicals within cotton have indicated that aggregation becomes dominant at loadings of $\gtrsim 10^{-2}$ mol kg^{-1}, when their concentration exceeds that of the pore sites available for adsorption.[53] The results reported here for Direct Blue 1 in cellophane indicate that aggregation becomes significant at a comparable loading (Figure 6; 1×10^{-2} mol dm^{-3} $\approx$ 0.8×10^{-2} mol kg^{-1}), suggesting that its onset may also be closely related to the number of sites available for strong dye−cellulose interactions.

Important practical applications of direct dyes are based on their binding to molecular surfaces provided by cellulose and by proteins. This study provides new information by quantifying the effect of dye aggregation within a cellulose environment: it indicates that the aggregation of Direct Blue 1 in cellophane becomes significant at loadings of $\gtrsim 10^{-3}$ mol kg^{-1} ($\gtrsim 10^{-3}$% w/w), which may have important implications for considering the reactivity of direct dyes on such surfaces.

Conclusions

The combined techniques of UV−visible, NMR, and resonance Raman spectroscopy have provided structural and thermodynamic information on dimer and trimer formation for the bis-azo dye, Direct Blue 1. The dimer and trimer form by stacking at the central biphenyl group to produce structures in which repulsion between the charged sulfonate groups is minimized; the process is driven enthalpically due to strong aromatic interactions between the biphenyl groups. The structure of the dimer in cellophane is similar to that in solution, with the lower driving force for dimerization within the nanopores being attributable to dye−cellulose interactions that compete effectively with dye−dye interactions. These conclusions for Direct Blue 1 may have wider implications for other dyes and their competitive intermolecular interactions, both between two dye molecules and between dye molecules and molecular surfaces.

Acknowledgment. We thank Ms. H. Fish and Ms. K. A. M. Ampt for measurement of NMR spectra. We acknowledge the support of Unilever Research.

Supporting Information Available: Aggregation analysis and application of exciton theory to a trimer. This material is available free of charge via the Internet at http://pubs.acs.org.

References and Notes

(1) Gregory, P. *High-Technology Applications of Organic Colorants*; Plenum: New York, 1991.

(2) *Chemistry and Technology of Printing and Imaging Systems*; Gregory, P., Ed.; Chapman & Hall: London, 1996.

(3) Zollinger, H. *Color Chemistry*; VCH: Weinheim, 1987.

(4) Ojala, W. H.; Ojala, C. R.; Gleason, W. B. *Antiviral Chem. Chemother.* **1995**, *6*, 25.

(5) Tsopelas, C.; Sutton, R. *J. Nucl. Med.* **2002**, *43*, 1377.

(6) Murakami, K. *Dyes Pigm.* **2002**, *53*, 31 and references therein.

(7) Monahan, A. R.; Blossey, D. F. *J. Phys. Chem.* **1970**, *74*, 4014.

(8) Monahan, A. R.; Germano, N. J.; Blossey, D. F. *J. Phys. Chem.* **1971**, *75*, 1227.

(9) Reeves, R. L.; Maggio, M. S.; Harkaway, S. A. *J. Phys. Chem.* **1979**, *83*, 2359.

(10) Hamada, K.; Take, S.; Iijima, T.; Amiya, S. *J. Chem. Soc., Faraday Trans. 1* **1986**, *82*, 3141.

(11) Skrabal, P.; Bangerter, F.; Hamada, K.; Iijima, T. *Dyes Pigm.* **1987**, *8*, 371.

(12) Hamada, K.; Mitshuishi, M.; Ohira, M.; Miyazaki, K. *J. Phys. Chem.* **1993**, *97*, 4926.

(13) Simončič, B.; Špan, J.; Vesnaver, G. *Dyes Pigm.* **1994**, *26*, 257.

(14) Tiddy, G. J. T.; Mateer, D. L.; Ormerod, A. P.; Harrison, W. J.; Edwards, D. J. *Langmuir* **1995**, *11*, 390.

(15) Murakami, K.; Kimura, Y.; Saito, M. *Bull. Chem. Soc. Jpn.* **1997**, *70*, 115.

(16) Iijima, T.; Jojima, E.; Antonov, L.; Stoyanov, S.; Stoyonova, T. *Dyes Pigm.* **1998**, *37*, 81.

(17) Dakiky, M.; Němcova, I. *Dyes Pigm.* **1999**, *40*, 141.

(18) Neumann, B. *Langmuir* **2001**, *17*, 2675.

(19) Neumann, B.; Huber, K.; Pollmann, P. *Phys. Chem. Chem. Phys.* **2002**, *2*, 3687.

(20) Yasunaga, T.; Nishikawa, S. *Bull. Chem. Soc. Jpn.* **1972**, *45*, 1262.

(21) Krässig, H. A. *Cellulose*; Gordon Breach Science Publishers: Amsterdam, 1993.

(22) Abbott, L. C.; Batchelor, S. N.; Jansen, L.; Oakes, J.; Lindsay Smith, J. R.; Moore, J. N. *New J. Chem.* **2004**, *28*, 815.

(23) Robinson, C.; Mills, H. A. *Proc. R. Soc. London, Ser. A* **1931**, *131*, 576.

(24) Schutte, W. J.; Sluyters-Rehbach, M.; Sluyters, J. H. *J. Phys. Chem.* **1993**, *97*, 6069.

(25) Toptygin, D.; Packard, B. Z.; Brand, L. *Chem Phys. Lett.* **1997**, *277*, 430.

(26) Dimicolli, J.-L.; Hélène, C. *J. Am. Chem. Soc.* **1973**, *95*, 1036.

(27) Camp, P. J.; Jones, A. C.; Neely, R. K.; Speirs, N. M. *J. Phys. Chem. A* **2002**, *106*, 10725.

(28) Malinowski, E. R. *Factor Analysis in Chemistry*, 3rd ed.; Wiley: New York, 2002.

(29) Abbott, L. C.; Paul, T.; Wight, P.; Lindsay Smith, J. R.; Moore, J. N., manuscript in preparation.

(30) Malinowski, E. R. *J. Chemom.* **1999**, *13*, 69.

(31) Colloidal aggregates of Direct Blue 1 ($n \gg 3$) have been reported under conditions of very high ionic strength,[32] and on "aging" of solutions,[9] but the evidence indicates that they were not present under the conditions used in the present study.

(32) Valkó, E. *J. Soc. Dyers Colour.* **1939**, *55*, 173.

(33) On one occasion, a fresh solution of Direct Blue 1 at 2×10^{-4} mol dm^{-3} without electrolyte gave a UV−visible spectrum that was similar to, but different from, that of the trimer calculated in Figure 2: the profile of this spectrum did not change on dilution to $<10^{-6}$ mol dm^{-3} at room temperature, but it reverted to that of a monomer sample on prolonged heating of the diluted sample at 60 °C. This sample may have contained colloidal aggregates produced by unintended seeding with particulate matter: we were unable to reproduce this result.

(34) *CRC Handbook of Chemistry and Physics*, 84th ed.; Lide, D. R., Ed.; CRC Press: Boca Raton, FL, 2003.

(35) The spectra recorded up to 50 °C give isosbestic points (Figure 3) that are consistent with a shift of the monomer−dimer equilibrium to the monomer form (Figures 1 and 2). These isosbestic points are lost as the temperature is raised further: the one at ca. 650 nm, on the long-wavelength side of the main band, is replaced at ca. 50−70 °C by a new isosbestic point at ca. 595 nm, on the short-wavelength side of this band. This observation is consistent with a shift from the ca. 100% hydrazone composition determined by NMR at 27 °C[22] to a mixture containing the azo form at these higher temperatures.[36]

(36) Joshi, H.; Kamounah, F. S.; van der Zwan, G.; Gooijer, C.; Antonov, L. *J. Chem. Soc., Perkin Trans. 2* **2001**, 2303.

(37) Steullet, V.; Dixon, D. W. *J. Chem. Soc., Perkin Trans. 2* **1999**, 1547.

(38) Kasha, M. *Radiat. Res.* **1963**, *20*, 55.

(39) Kasha, M.; Rawls, H. R.; Ashraf El-Bayoumi, M. *Pure Appl. Chem.* **1965**, *11*, 371.

(40) López Arbeloa, I. *J. Chem. Soc., Faraday Trans. 2* **1981**, *77*, 1725.

(41) López Arbeloa, F.; Ruiz Ojeda, P.; López Arbeloa, I. *J. Chem. Soc., Faraday Trans. 2* **1988**, *84*, 1903.

(42) López Arbeloa, F.; Herrán Martínez, J. M.; López Arbeloa, T.; López Arbeloa, I. *Langmuir* **1998**, *14*, 4566.

(43) López Arbeloa, F.; Martínez Martínez, V.; Bañuelos Prieto, J.; López Arbeloa, I. *Langmuir* **2002**, *18*, 2658.

(44) The fits were made with the minimum number of bands. An alternative approach would involve additional vibronic bands but would require relatively arbitrary guesses of their parameters. The band-fitting analysis is performed to estimate geometric parameters of the dimer and trimer: these estimates are relatively insensitive to small changes in the detail of the band-fitting analysis, as discussed below.[45,47]

(45) For example, for the $I = 0.1$ analysis, $\theta = 82-86°$ is obtained for $f_1/f_2 = 0.70-0.80$ with other parameters unchanged.

(46) For an oblique geometry with the calculated angle and separation, the two molecules would physically overlap if the transition dipole were to lie along the long molecular axis, and the two halves of the molecule would be inequivalent; if the transition dipole were to lie along the short molecular axis, they would be widely separated, with a similarly weak degree of interaction along the whole molecule.

(47) For example, for the $I = 0.1$ analysis, $R = 5.8-4.6$ Å is obtained for the sandwich model with $\theta = 82-86°$ and other parameters unchanged; $R = 3.4-5.2$ Å is obtained for the offset sandwich model with $\phi = 81-90°$, $\theta = 84°$, and other parameters unchanged (i.e., $\phi = 90°$ gives the limiting case of no offset; see Table 2).

(48) Tsuzuki, S.; Tanabe, K. *J. Phys. Chem.* **1991**, *95*, 139 and references therein.

(49) Skowronek, M.; Stopa, B.; Konieczny, L.; Rybarska, J.; Piekarska, B.; Szneler, E.; Bakalarski, G.; Roterman, I. *Biopolymers* **1998**, *46*, 267.

(50) Müller-Dethlefs, K.; Hobza, P. *Chem. Rev.* **2000**, *100*, 143.

(51) Hunter, C. A.; Lawson, K. R.; Perkins, J.; Urch, C. J. *J. Chem. Soc., Perkin Trans. 2* **2001**, 651.

(52) Lee, N. K.; Park, S.; Kim, S. K. *J. Chem. Phys.* **2002**, *116*, 7910.

(53) Scheuermann, R.; Roduner, E.; Batchelor, S. N. *J. Phys. Chem. B* **2001**, *105*, 11474.